Can Terrestrial Laser Scanner (TLS) and hemispherical photographs predict Tropical Dry Forest Succession with liana abundance?

G. Arturo Sánchez-Azofeifa[a*], Mauricio Vega-Araya[b], J. Antonio Guzmán[a], Carlos Campos-Vargas[a], Sandra M. Durán[a], Nikhil D'Souza[a], Thomas Gianoli[a], Carlos Portillo-Quintero[c], Iain Sharp[a]

[a] Center for Earth Observation Sciences (CEOS), Department of Earth and Atmospheric Sciences, University of Alberta, Edmonton, Alberta, Canada T6G 2E3

[b] Laboratorio de Teledetección de Ecosistemas (LabTEc), INISEFOR-Universidad Nacional de Costa Rica, Heredia, Costa Rica, Central America

[c] Department of Natural Resources Management, Texas Tech University, Lubbock, Texas, USA.

[*] Corresponding author. Tel. +1-780-4921822; E-mail address:gasanche@ualberta.ca

Abstract

Tropical Dry Forests (TDFs) are ecosystems with long drought periods, a mean temperature of 25^{o}C, a mean annual precipitation that ranges from 900 to 2000 mm, and that possess a high abundance of deciduous species (trees and lianas). What remains of the original extent of TDFs in the Americas remains highly fragmented and at different levels of ecological succession. It is estimated that one of the main fingerprints left by global environmental and climate change in tropical environments is an increase in liana coverage. Lianas are non-structural elements of the forest canopy that eventually kill their host trees. In this paper we evaluate the use of a Terrestrial Laser Scanner (TLS) in combination with hemispherical photographs (HPs) to characterize changes in forest structure as a function of ecological succession and liana abundance. We deployed a TLS and HP system in 28 plots throughout secondary forests of different ages and with different levels of liana abundance. Using a canonical correspondence analysis, we addressed how the VEGNET and HPs could predict TDF structure. Likewise, using univariate analysis of correlations we show how the liana abundance could affect the prediction of the forest structure. Our results suggest that TLS and HPs can predict differences in the forest structure at different successional stages, but that these differences disappear as liana abundance increases. Therefore, in well-known ecosystems such as the tropical dry forest of Costa Rica, these biases of prediction could be considered as structural effects of liana presence. This research contributes to the understanding of the potential effects of lianas in secondary dry forests and highlights the role of TLS combined with HPs to monitor structural changes in secondary TDFs.

1 Introduction

Lianas, woody vines, are a key structural component of tropical forests; they account for 25–40% of the woody stems and more than 25% of the woody species (*Schnitzer and Bongers, 2011*). Lianas are structural parasites that use trees to ascend to the forest canopies, and as such can be detrimental to host trees by competing with them for above- and belowground resources (*Chen et al., 2008*), reducing tree growth rates, and increasing tree mortality (*van der Heijden et al., 2013*). Thus, lianas are able to reduce carbon storage and uptake in old-growth tropical forests (*Durán and Gianoli, 2013; van der Heijden et al., 2015*).

Lianas have been defined as hyper-dynamic elements of the canopy structure (*Sanchez-Azofeifa and Castro, 2006*). In the last two decades lianas have increased in density and biomass in old-growth forests (*Phillips et al., 2002; Schnitzer and Bongers, 2011*), and this increment is considered to be one of the major structural changes in tropical forests (*Phillips and Lewis, 2014*), because it can have potential negative effects on carbon stocks. Liana dynamics in secondary forests, however, are not yet understood despite the fact that secondary forests are becoming increasingly dominant in tropical regions, and currently occupy more area than old-growth forests (*Durán and Sánchez-Azofeifa, 2015; Wright, 2005*).

Lianas are considered light-loving plants, because they tend to respond positively to disturbance and show high density in areas of secondary forest succession (*Paul and Yavitt, 2011*). Secondary forests may promote liana abundance because they provide both high light availability and an abundance of trellises (*Schnitzer and Bongers, 2002*). In treefall gaps, lianas can form dense tangles and reduce the amount of light reaching the forest understory

(*Paul and Yavitt, 2011; Schnitzer et al., 2000*). These liana tangles can persist for long periods (up to 13 years) and alter the successional pathway to one(?) stalled by liana abundance by inhibiting the regeneration, growth, and density of late successional species (*Schnitzer et al., 2000*).

As of today, it is still unknown whether lianas can alter successional trajectories in secondary forests resulting from anthropogenic disturbance (*Durán and Sánchez-Azofeifa, 2015*). Two studies in secondary wet forests have found an increment in liana density in the first 20 years of regeneration (age since land abandonment), with a subsequent decline (*DeWalt et al., 2000; Letcher and Chazdon, 2009*). This decline of lianas in wet forests appears to be related with reductions in light availability due to greater tree and shrub biomass at later stages of succession (*Letcher and Chazdon, 2009*). Nonetheless, it remains unclear whether this pattern holds true with more open forest types, and whether other factors such as structure, canopy openness, plant density and the volume of forest stands can also influence successional trajectories of lianas (*Durán and Sánchez-Azofeifa, 2015; Sánchez et al., 2009*).

Assessments of forest structure in different stands are often constrained by accessibility, and the cost of personnel and equipment. Remote sensing offers an efficient alternative to detect changes in vegetation and examine how lianas may change across stands with different structures. Nonetheless, few studies have assessed the potential of remote sensing (space-borne or airborne) to detect the presence of lianas in tropical forests with the objective of providing tools to map their extent from local to landscape level, and measure their ecological footprint (*Foster et al., 2008*). *Sanchez-Azofeifa et al*. (*2009*) used hemispherical photography over a succession of tropical dry forests and found that lianas

85 contributed substantially to forest-level Wood Area Index (WAI). Other studies found
86 differences between the biochemical, structural and hyperspectral properties of lianas and
87 trees in tropical dry forests (*Castro-Esau et al., 2004; Sanchez-Azofeifa et al., 2009*). These
88 studies emphasized the potential of using remote sensing to map liana abundance at regional
89 scales. However, given the important effect of lianas on the biomass distribution within
90 tropical forests (*Schnitzer and Bongers, 2011*), remote sensing tools capable of measuring
91 the vertical distribution of biomass within tropical forests are probably more adequate for
92 detecting the presence and variation of liana density across forest stands.

93 Terrestrial Laser Scanners (TLS) have demonstrated their capability to measure canopy
94 properties such as height and cover (*Ramírez et al., 2013*) and tree architecture (*Lefsky et al.,*
95 *2008*), (*Dassot et al., 2011*; *Richardson et al., 2014*). In the last decade, there has been a rapid
96 development in portable TLS (*Dassot et al., 2011; Richardson et al., 2014*). When laser
97 pulses emitted in the visible or near-infrared come into contact with an object, part of that
98 energy is reflected back toward the instrument which triggers the recording of its distance
99 and intensity (*Beland et al., 2014*). TLS systems typically employ vertical and horizontal
100 scanning around a fixed point of observation, providing a hemispherical representation of
101 biomass distribution in the forest -leaves, branches and trunks- which allows for the
102 exploration of foliage angle distributions and clumping (*Clawges et al., 2007; Jupp et al.,*
103 *2009; Strahler et al., 2008*).

104 Until today, there has been no concrete evidence about how liana abundance can
105 affect the prediction of the forest structure by TLS or HPs (HPs). Because of this, the
106 objective of this study was to evaluate the feasibility of a TLS named VEGNET in
107 combination with HPs to assess changes in forest structure in secondary TDFs with different

levels of lianas abundance. The VEGNET is a TLS that automatically scans a forest plot producing a vertical foliage density profile. Given its automated mode of operation and semi-permanent installation, the VEGNET instrument is described as an *in situ* Monitoring LiDAR (IML) (*Culvernor et al., 2014; Portillo-Quintero et al., 2014*).

As such, in this paper we first assess the potential of VEGNET and HPs to detect the vertical structure of forest stands at different successional stages. Second, we examine how liana abundance could affect the bias of prediction of VEGNET and HPs to detect the level of succession of a given forest stand. Therefore, in well-known ecosystems such as the tropical dry forest of Costa Rica, this bias of prediction could be considered as the effect of liana presence on forest structure.

2 Methods

2.1 Study Area

The study area is located in the Santa Rosa National Park Environmental Monitoring Super Site (SRNP-EMSS), which is a part of the Guanacaste Conservation Area in Costa Rica (10°48" N, 85°36" W) (Figure 1). This site covers an area of 50,000 ha, receives 1720 mm of annual rainfall, has a mean annual temperature of 25°C and a 6-month dry season (Dec–May)

(*Kalácska et al.,2004*). The SRNP-EMSS site has suffered intense deforestation in the past 200 years due to the expansion of pasturelands (Calvo-Alvarado et al., 2009). Original land management practices in the park included pasture rotation between different large corrals surrounded by life fences that can still be identified today. More recently (early 1970's) with the creation of Santa Rosa National Park, a process of secondary regeneration has become

131 the dominant land cover change force in the region. Today and after the creation of SRNP,
132 the uplands of the park are a mosaic of secondary forest in various stages of regeneration
133 and with different land use histories related to anthropogenic fires, intense deforestation, and
134 clearing for pasture lands (*Kalácska et al., 2004; Arroyo-Mora et al., 2005a, Sen et al,*
135 *2015*).
136
137 **2.2 Definition of forest cover and plot age.**
138 A map of forest cover and forest cover ages was generated using aerial photographs
139 collected by the US Army in 1956 (Scale 1:24,000), a Multispectral Scanner (MSS) image
140 from 1979 (80 m spatial resolution); 4 Landsat Thematic Mapper [TM] images from 1986,
141 1997, 2000 and 2005 (28.5 m spatial resolution); one Spot Multispectral image from 2010
142 (20 m spatial resolution); and a Landsat 8 image from 2015. All images had less than 10%
143 cloud cover.
144 The 1986 image was georeferenced to 1:50,000 topographic maps from the Costa Rica
145 National Geographic Institute with a Root Mean Square Error (RSME) of 0.5 pixels or 14.25
146 m. We defined this as our master image in order to georeference all of the other images, as
147 such all other images were then geo-referenced to the 1986 image seeking a RMSE close to
148 0.5 pixels between the master and the target image. All images where then classified using a
149 supervised classification. Image accuracy was conducted for the 1997, 2000, 2005 and 2010
150 satellite images as part of independent validation efforts conducted by the Costa Rica's
151 National Forest Financing Fund (FONAFIFO). Overall accuracy for the forest/non-forest
152 images was 90%. Further information on image processing can be found in Sanchez-
153 Azofeifa et al. (2001).

Final quality controlled forest cover maps (forest non-forest) for 1956, 1979, 1986, 1997, 2000, 2005, 2010 and 2015 were cross referenced to produce a tropical dry forest age map. Specifically, forest coverage with 60 years old correspond to woodlands which were being observed in images since 1956; forests that were 40 years old were not detected in 1956 but have been recognizing as forests since 1979; on the other hand, woodlands that were referred to as being 10 years old have a minimum of 10 years as a discriminable forest coverage. Based on Arroyo-Mora et al (2005) and Kalascka et. al's (2005) studies the following successional classification was developed: Ages 10 to 40 years (Early), and ages 40 to 60 (Intermediate). Figure 1 presents the final land cover and forest age map for our study area. Figure 1 presents the final land cover and forest age map for our study area.

2.3 Plots selection and description

Based on Figure 1, twenty-eight randomly stratified 0.1ha plots were selected. The number of plots chosen for each forest successional stage was based upon each stages total forest cover area. Plot sizes of 0.1 ha follows convention used in tropical forest studies at this site (Kalascka et al. 2005). Fieldwork conducted in July 2016 was conducted in order to characterize diameter at breast height (DBH), tree height, total biomass, VEGNET observations (canopy vertical profiles) and hemispherical photos (Canopy openness and Leaf Area Index).

The characterization of successional stages was performed following previous approaches for seasonally dry forests of Costa Rica (*Arroyo-Mora et al., 2005b; Kalácska et al., 2005*) and adjusted according to the estimated forest ages (Figure 1). These approaches categorized the secondary regeneration in different successional stages such as early and intermediate successional stages (*E* and *I*, respectively) (*Arroyo-Mora et al., 2005a*). The *E* stage is a

177 forest area with patches of sparse woody vegetation composed of shrubs, small trees, and
178 saplings, with a thick herbaceous understory, and with a single stratum of tree crowns with a
179 maximum height of less than 10 m (*Castillo et al., 2012*). Some of the common species that
180 are characteristic of this early stage of succession includes *Genipa americana*,
181 *Cochlospermum vitifolium*, *Gliricidia sepium*, *Randia monantha* (*Hilje et al., 2015;*
182 *Kalácska et al., 2004*). In contrast, the *I* stage has two vegetation strata composed of
183 deciduous species of woody plants. The first strata is comprised of fast-growing deciduous
184 tree species that reach a maximum height of 10–15 m (e.g., *Cydista aequinoctialis*) and the
185 second stratum is represented by lianas and vines, adults of shade-tolerant and slow-growing
186 evergreen species as well as the juveniles of many species such as *Annona reticulata*,
187 *Ocotea veraguensis*, and *Hirtella racemosa* (*Arroyo-Mora et al., 2005a; Kalácska et al.,*
188 *2004*). No lianas were present in the early successional stage plots. Lianas in early forests
189 tend to be present more later in the succession, specifically in the transition from early to
190 intermediate stages. We did not select "late forests" since they tend to reflect the
191 characteristics of tropical moist forests with significant structural characteristics very
192 different from true late tropical dry forests sites (Tosi, personal communication).
193 On the other hand, the characterization of the plots according to the liana abundance was
194 based on the structure of plants that compose the tropical dry forest of SRNP-EMSS. In this
195 way, we classified the 28 plots according to the relative abundance of stems of lianas, where
196 plots with a relative abundance greater than 0.1 were categorized as plots having high liana
197 abundance (HL), while plots with a relative abundance lower than 0.1 were categorized as
198 having a low liana abundance (LL). Although this classification seems to be in-
199 deterministic, this kind of classification represents an important ecological component which

200 is very difficult to study as a continuum due to its spatial and temporal variation, and its
201 categorization can help to improve the understanding of ecological processes as many other
202 ecological categories.
203 At the end of this characterization, we used 11 *E* plots and 17 *I* plots, with 12 of those
204 plots being LL and the other 16 plots being HL. Altogether, ours plots for the study
205 consisted of 5 *E*-LL plots, 6 *E*-HL plots, 7 *I*-LL plots, and 10 *I*-HL plots. In each of these
206 plots we extracted the available information that described the complexity of the dry forest
207 according to its structure, but at the same time deployed the ground LiDAR and
208 hemispherical photograph measurements to predict and describe that complexity.
209 Information about the parameters used and estimated according to the forest structure,
210 ground LiDAR, and hemispherical photographs is described below.
211
212 **2.4 Forest structure**
213 Four parameters that characterize the forest structure were used in this study. These
214 parameters were selected because these are easily obtained in any forest inventory, which
215 could help in the applicability of this study in other regions. Specifically, we selected the
216 stem density (stems/ha) as a parameter to describe the number of individuals per plot, the
217 mean diameter at breast height (1.3 m) (DBH_{mean}, cm) as a parameter that can describe the
218 mean size of the individuals, the total basal area (TBA, m^2) as a parameter that can describe
219 the biomass of each plot, and the ratio of liana basal area to TBA (L/TBA) as a parameter
220 that can describe the contribution of lianas biomass to the total biomass of each plot. Each
221 of these parameters was extracted from DBH measurements for lianas (>2.5 cm) and trees
222 (>5 cm).

223

224 **2.5 Ground LiDAR measurements**

225 The VEGNET ground LiDAR system was deployed in the middle of each of the selected
226 plots, in which a single successful scan was performed between June 12th to June 27th, 2016.
227 The VEGNET IML instrument uses a phase-based laser rangefinder with a wavelength of
228 635 nm, in which a laser beam is directed at a rotating prism that reflects the laser at a fixed
229 angle of 57.5° zenith or the "hinge angle" (*Jupp et al., 2009*). The prism is designed to
230 perform full 360° azimuth rotations at this fixed zenith angle (no vertical scanning motion)
231 and has the capability to be programmed to obtain up to 7360 range measurements for a full
232 azimuth scan (an average of 20.6 measurements per azimuth degree) (*Culvenor et al., 2014*).
233 Because sunlight irradiance may cause interference with the VEGNET laser at the same
234 wavelength (*Culvenor et al*., 2014, *Portilllo-Quintero et al*., 2014), measurements for the
235 VEGNET were conducted at night. Some tests of the measurement process by VEGNET at
236 night time indicated that at distances greater than 60 m or in areas larger than 3600 m^2 (0.36
237 ha) the laser beam does not provide reliable measurements (*Culvenor et al., 2014*). In a
238 tropical forest setting, data analysis and interpretation may be restrained to the footprint,
239 which is dependent on forest height at each site. Based on the forest heights of our study
240 sites, the effective footprint of LiDAR measurements was within 0.1ha of our original
241 sampling area.

242 From these measurements at night six parameters were estimated: the maximum tree
243 height (H_{max}), the plant area index (PAI), plant area volume density (PAVD), the centroid of
244 x (C_x) and y (C_y), and the radius of gyration (RG). To estimate these parameters, the height
245 (h) was initially calculated as the cosine of the laser zenith angle (57.5°) multiplied by the

246 laser distance measurement (*d*) assuming that the terrain is flat as describe *Culvenor et al.*
247 (*2014*).
248 On the other hand, canopy "hits" and "gaps" were recorded to enable the calculation
249 of angular gap fraction or gap probability (P_{gap}) at each *h* where a leaf, trunk or branch was
250 hit by the laser (*Lovell et al., 2003*). P_{gap} at a given *h* is the ratio of the number of valid
251 returns below *z* ($\#z_i < h$) to the total number of laser shots (*N*) (*Culvenor et al., 2014*):
252 $$P_{gap(z)} = [\#z_i < h\ ] / N \quad (1)$$
253 Consequently, the estimation of cumulative plant area index (PAI) by the conversion of
254 $P_{gap(z)}$ was performed using the following the equation (*Culvenor et al., 2014*):
255
256 $$PAI_{(z)} = -1.1 \times \ln(P_{gap(z)}) \quad (2)$$
257
258 From this calculation, the density of vegetation components at any level of *z* was
259 computed as the derivative of PAI with respect to *h*. This calculation is commonly referred
260 to as the plant area volume density (PAVD) (*Culvenor et al., 201*) described by:
261
262 $$PAVD_{(z)} = \delta\ PAI_{(z)} / \delta_z \quad (3)$$
263
264 It is important to note that these calculations represent tridimensional variations (x, y,
265 z) of the forest structure (*Culvenor et al., 2014*), because of this, in our statistical analysis
266 we used the maximum *h* estimated by the LiDAR per plot (H_{max}), the cumulative PAI as a
267 function of the canopy height (PAI), and the mean PAVD at different heights ($PAVD_{mean}$).

These calculations were extracted using the "VEGNET Data Display and Export Version 2.5" software developed by Environmental Sensing Systems Inc (Melbourne, Australia).

Likewise, from the LiDAR measurements we also used shape metrics such as the centroid (*C*) and radius of gyration (RG) to understand how the vertical profile of the forest could change according to successional stages and liana abundance. The RG and the *C* are metrics that are mainly used in LiDAR waveforms to describe the motion of objects and the manner in which material is distributed around an axis (*Muss et al., 2013*). We used a similar approach by calculating the *C* and the RG for the PAVD vertical profile of each plot. Specifically, *C* represents the geometric center of a two-dimensional (*x* and *y*) region (e.g., the arithmetic mean position) of all the points (*n*) in the shape of the PAVD profile, while RG is the root mean square of the sum of the distances for all points on the PAVD vertical profile, which is described as:

$$RG\sqrt{\frac{\sum(x_i-c_x)^2+\sum(y_i-c_y)^2}{n}} \quad (4)$$

This parameter can be visualized as the relationship between the total length of the PAVD vertical profile and its shape and position, which are determined using the sum of *x* or *y* coordinates divided by the total length of the profile (*Muss et al., 2013*). In general, the RG captures the manner in which the PAVD profile is distributed around the centroid, making it a better descriptor of the vertical profile shape than just the centroid itself, and thus, more suitable for relating VEGNET measurements to forest structure (*Muss et al., 2013; Culvenor et al., 2014*). Therefore, we used the RG to relate the shape of the PAVD profile to forest biomass at the footprint level For a more detailed explanation on the functioning of the VEGNET in the field please refer to *Portillo-Quintero et al*. (*2014*) as

291 well as *Culvenor et al.* (*2014*). A single successful scan was performed during the wet
292 season using the VEGNET instrument at each site on clear nights.
293
294 **2.6 Hemispherical photographs**
295 Hemispherical photographs (HPs) were taken during the early morning in the middle of each
296 plot, using a digital camera (E4500, Nikon, Tokio, Japan) equipped with a fisheye lens of 35
297 mm focal length. The camera was leveled at 1.50 m by a tripod and orientated towards
298 magnetic north, in order to ensure photographic standardization.. The resulting pictures were
299 analyzed using the software Gap Light Analyzer version 2.0.4 (*Frazer et al., 1999*). This
300 analysis was performed by creating 340 sky sectors (36 azimuth classes and 9 elevation
301 angle classes) with a time series of 2 min along the solar track. The leaf area index (LAI)
302 and the canopy openness were subsequently extracted by this analysis; however, the LAI
303 was extracted using the "4 ring" which is a more accurate depiction of the site than using "5
304 rings" because the latter takes into account trees that are not immediately surrounding the
305 site, and which are found outside of the plot footprint.
306
307 **2.7 Statistical analysis**
308 This study compared the effect of the successional stages, the abundance of lianas, and their
309 interaction on the parameters of forest structure as well as VEGNET-HPs parameters using a
310 multivariate analysis of variance (MANOVA), in order to demonstrate that this study had
311 been conducted in contrasting environments. For each MANOVA we extracted the
312 univariate analysis of variance (ANOVA) to describe the multivariate effects of each
313 parameter. To show the potential of the VEGNET and HPs to predict variations in the

314 structure of the dry forest, we applied a canonical correlation analysis (CCA) using the
315 VEGNET-HPs parameters as independent variables and the features of the forest stand as
316 dependent variables. Due to the CCAs sensitivity to the collinearity among variables (*Quinn*
317 *and Keought, 2002*), we only used RG, PAI, $PAVD_{mean}$, H_{max}, LAI, and canopy openness as
318 independent parameters. Specifically, the CCA was used to extract the canonical correlation
319 between VEGNET-HPs and forest structure (eigenvalues), the correlation between the
320 canonical variates and each matrix (eigenvectors), and the scores that describe the
321 multidimensional variation of each plot according to its correlation. To extract the statistical
322 significance of the canonical correlation coefficients, we computed an asymptotic test on the
323 first canonical dimensions to extract the *F*-approximations of Wilks' Lambda along with its
324 significance. This statistical significance was subsequently validated using a permutation
325 test on each dimension by 10000 iterations.

326 After describing the potential of the VEGNET-HPs parameters to predict variations
327 in the structure of the dry forest, we were interested in demonstrating how the relative
328 abundance of lianas could affect the bias of prediction extracted from these sensors. In
329 ecological terms, it is a perceived expectation that during successional transitions increases
330 in basal area, height and vertical strata of the vegetation should be observed; consequently,
331 these transitions could be translated into increases in VEGNET-HPs parameters (except
332 canopy openness which is inverse). However, from hypothesis derived from previous
333 studies, it is possible that the abundance of lianas may actually arrest the forest succession
334 and reduce the biomass accumulation of woody vegetation (*Paul and Yavitt 2011; Schnitzer*
335 *et al., 2000*). If the above is true, correlations between descriptors of forest structure and
336 parameters extracted from VEGNET and HPs could be diffuse or stochastic in the dry forest,

and their application under the presence of lianas could prove ineffective. Under this reasoning, we compare the parametric correlations of four parameters according to the successional stages and the liana abundance, separately. The four parameters selected were those with the two highest eigenvalues for the VEGNET-HPs matrix and the two parameters with the highest eigenvalue for forest structure, determined by the first two canonical dimensions described by the CCA. This comparison was conducted using an ordinary resampling method to replicate the correlation 5000 times, in which the resampled values were used to build density plots to describe the bias of prediction according to its overlap.

The previous analyses were conducted in R software version 3.3.1 (R Development Core Team, 2016) using the "CCA" package (*González and Déjean, 2015*) to extract the canonical correlations, the "CCP" package (*Menzel, 2009*) to extract the significance of the CCA and its permutation, and the "boot" package (*Canty and Ripley, 2016*) to extract the resampled values. When the normality of the data was not reached, each parameter was previously transformed using the Box-Cox transformation for the analysis.

3 Results

3.1 Forest structure

According to the MANOVA the forest structure of the plots differed between successional stages (Wilk's $Lambda_{(4,21)} = 0.51$; $p < 0.01$) and liana abundance (Wilk's $Lambda_{(4,21)} = 0.58$; $p < 0.05$), but without interaction between these categories (Wilk's $Lambda_{(4,21)} = 0.76$; $p = 0.20$) (Table 1). This analysis suggests that the DBH_{mean} and TBA were the only parameters affected by the interaction between successional stages and liana abundance, where *E* successional plots with LL and *I* plots with HL showed lower values of DBH_{mean}

and TBA than *E* and *I* plots with HL and LL, respectively. In terms of the effect of the liana abundance, the univariate analysis suggests that plots with LL showed lower values of L/TBA in comparison with HL plots.

3.2 VEGNET-Hemispherical Photographs (HPs)

The multivariate comparisons of the VEGNET-HPs parameters showed that the sensor estimations did not differ between successional stages (Wilk's $\text{Lambda}_{(8,17)} = 0.58$; $p = 0.21$), liana abundance (Wilk's $\text{Lambda}_{(8,17)} = 0.62$; $p = 0.29$), and these categories did not show an interaction (Wilk's $\text{Lambda}_{(8,17)} = 0.53$; $p = 0.14$) (Table 2). Despite the absence of a multivariate effect of the liana abundance, the univariate responses extracted from this comparison suggest that the LAI and canopy openness differs between plots with HL and LL, where LL plots showed lower values of LAI and higher values of canopy openness in comparison with HL plots (Table 1). On the other hand, the univariate responses showed that the canopy openness was affected by the successional stages, where *E* successional plots showed higher values of canopy openness than *I* plots. Likewise, the univariate comparisons suggest that C_x, PAI, and $\text{PAVD}_{\text{mean}}$ are affected by the interaction of the successional stages and liana abundance, where *E* successional plots with LL and *I* plots with HL showed higher values of C_x, PAI, and $\text{PAVD}_{\text{mean}}$ in comparison with *E* and *I* successional plots with HL and LL, respectively.

3.3 Canonical correspondence analysis

The CCA showed that sensor parameters are strongly associated with the trends in forest structure (Fig 2). In general, the first and second canonical dimension showed correlations of

383 0.81 (Wilk's Lambda$_{(24,64.01)}$ = 0.13; $p < 0.01$) and 0.72 (Wilk's Lambda$_{(15,52.85)}$ = 1.46; p =
384 0.16) between our sensors and forest structure. Specifically, the correlation between the
385 canonical variates in the first canonical dimension suggested that canopy openness and the
386 LAI have a great weight in the sensor matrix, while L/TBA and stem density had an
387 important effect on the forest structure (Fig 2a). Likewise, the correlation between the
388 canonical variates in the second canonical dimension showed that H_{max} and PAVD$_{mean}$ had a
389 strong correlation with the sensor parameters, while TBA and steam density had a strong
390 correlation on the forest structure. The scores that described the multidimensional variation
391 of each plot did not reflect a visual aggregation according to the successional stages and
392 liana abundance (Fig. 2b). In terms of the validation of the significance of the canonical
393 correlation coefficients, the permutations test showed that there is an important increase in
394 the significance of the first two canonical dimensions (Fig. 2c, 1d), where the first
395 dimension presented an increase of 0.21 points for the Wilks's statistic, while the second
396 dimension showed an increase of 0.25 points, which results in a significant effect.
397
398 **3.4 Comparison of correlations between successional stages and liana abundance**
399 The different trends of correlation showed that the successional stages and mainly the liana
400 abundance have an important effect in the prediction of the forest structure using VEGNET-
401 HPs parameters (Figure 3), but at the same time, these trends showed that some of these
402 parameters have the potential to predict the implication of the liana abundance on the forest
403 structure. Specifically, variation in the correlations of canopy openness on L/TBA (Figures
404 3a, b, c) and H_{max} on TBA (Figures 3g, h, i) showed that the correlation trends between
405 successional stages are overlapped, while the correlations trends between liana abundance

406 are separated, in where low values of canopy openness and H_{max} are associated with high
407 values of L/TBA and TBA, and consequently with the discrimination of HL plots. Likewise,
408 variation in the correlation between LAI and L/TBA showed that the trends might not be
409 used to separate successional stages or liana abundance (Figures 3d, e, f). However, the
410 correlation between H_{max} and TBA suggest that H_{max} can not discriminate between different
411 successional stages, but can discriminate with different liana abundance (Figures 3j, k, l),
412 where high values of correlation are associated with intermediated and HL plots.
413
414 **4 Discussion**
415 Woody vines or lianas tend to proliferate in disturbed forest stands such as
416 regenerating forests (*Paul and Yavitt, 2010*). Much research on liana ecology, however, has
417 focused on old-growth forests despite that secondary forests currently cover a larger area
418 than old-growth forests and may become the dominant ecosystem in tropical regions
419 (*Wright, 2005*). Due to shorter stature and a higher varilability of light in secondary forests,
420 lianas may be particularly abundant in these ecosystems, but little is understood about the
421 role of lianas in forest succession (*Letcher and Chazdon, 2009*). In this study, we used the
422 VEGNET, a terrestrial LiDAR system combined with HPs, to assess the impact of liana
423 abundance on forest succession. Our overall analysis first indicated that VEGNET
424 parameters in combination with HPs derived information was able to characterize changes in
425 forest structure at different successional stages. This finding in fact is not new, and it has
426 been demonstrated previously in the literature for other TDFs across the Americas including
427 the SRNP-EMSS (Sanchez-Azofeifa et al, 2009) when the effect of lianas is ignored. In fact,
428 it should be normal to expect some sort of correlation between forest succession and changes

on structural parameters since many parameters such as biomass, LAI, Canopy Openess and H_{max} will change as trees grow during the successional process. The fundamental difference occurs when lianas are integrated into the successional system.

When we consider the bias of correlations between the forest structure and the parameters extracted from our two sensors at different successional stages, as well as liana abundance, our results suggest that this late variable has an important effect on the bias of prediction for a given forest structure. The main reason is probably a result of lianas introducing random tangles into the 3-dimensional space that is occupied by all forest biomass at a given plot. In other words, lianas tend to randomize a space typically utilized by trees, which in the absence of lianas would be occupied deterministically by trees. This randomization of the 3D space occupied by trees and lianas is an element that has not been considered as of today; since most studies do not consider the space occupied by lianas because of a lack of TLS information.

This change in deterministic patterns of the forest structure is probably due to competition between lianas and trees in forest stands within a random 3D space. In disturbed sites, such as secondary forests, lianas deploy leaves in the canopy and create large amounts of tangles in both the ground and mid canopy, in order to reduce the amount of light available as well as the amount of incoming solar radiation available for photosynthesis for other plant species (*Graham et al., 2013*). Moreover, in regenerating stands within forests (e.g., treefall gaps), high densities of lianas can inhibit the regeneration of tree species and reduce the abundance of shade-tolerant trees (*Schnitzer et al., 2000*), which in turn can affect the 3D arrangement of species within a given area. These ecological processes may cause a shift in forest structure, which is detected as a shift in the vertical structure signature by TLS

452 in sites with high liana abundance. These differences in structures have been confirmed in a
453 recent study, which found that a liana-infested forest had a more irregular canopy with
454 canopy heights between 10 and 20 m, while the surrounding forests had a significantly taller
455 canopy between 25 and 35m along with a denser canopy (*Tymen et al., 2016*).
456 The information provided in this paper is clear in the sense that some variations in
457 the TLS and hemispherical camera parameters can be used to estimate the impact of lianas
458 on forest structure along the path of succession, although not all of parameters were
459 significant. In other words, there is a strong need to carefully select which parameters should
460 be considered if we want to estimate changes in the forest structure as function of liana
461 abundance. One key example is the use of PAI as tool to evaluate the impact of liana
462 abundance on forest succession. PAI as a single measurement theoretically could provide
463 insights on the impact of liana abundance on successional stages. Theoretically we could
464 expect that PAI will increase as leaf and wood biomass increase during succession (*Quesada*
465 *et al., 2009*). It is surprising that we did not find differences in the PAI values between
466 stands that did and did not have. It is possible that PAI is not the best parameter to
467 differentiate between plots with and without liana presence, instead variables more related
468 with leaf components, such as leaf area index (LAI) may be more suitable for finding
469 differences in liana signature across sites, especially when the contribution of lianas to the
470 woody area index (WAI) to overall plot PAI is relatively small in comparison to the
471 allocation of WAI from trees (*Sanchez-Azofeifa et al., 2009*).
472 A recent study assessing the role of lianas on forest dynamics in the Amazon,
473 indicated that a liana-infested forest appeared to be in an arrested stage of ecological
474 succession, due to the evidence provided by LiDAR surveys from 2007 to 2012 which

showed that the overall extent of forest area had remained stable, with no notable net gain or loss over the surrounding forest (*Tymen et al., 2016*). It is possible that studying forest dynamics in forest stands across successional stages, with different levels of liana abundance integrated into the TLS and HPs parameters, may allow us in the future to provide stronger evidence as to whether lianas can arrest succession in dry forests as it appears to occur in humid forests (*Schnitzer et al., 2000; Tymen et al., 2016*).

5 Conclusions

This study evaluated the potential for TLS and hemispherical photos to observe differences between successional stages of a tropical dry forest chrono-sequence and liana abundance. Our work provided five main conclusions: (1) that TLS data combined with hemispherical photography data can help to predict the forest structure of the tropical dry forest as demonstrated before, (2) that these predictions get blurry when liana abundance is considered, (3) that variations in TLS and HPs parameters can be used to predict the effect of liana abundance on the successional path, (4) that not all the parameters could address the effect of the presence or impact of lianas along a successional gradient, and (5) we suggest that the impact of lianas on successional stages changes the deterministic nature of forest structure, by randomizing the 3D space where they grow at given plot; the higher the abundance of lianas the higher the randomization.

Our study provides important insights on the contributions of lianas to the successional process, and highlights the potential that TLS has in monitoring liana presence in tropical dry forests environments. Lianas are increasing in density and biomass in tropical forests, but it is unknown whether this pattern is also found in secondary forests, which are

498 suitable for liana proliferation. TLS systems are capable of providing unbiased estimations
499 for the vertical structure of a given site, and thus constitute a powerful tool to monitor the
500 increases in liana density and biomass. Although, our study is limited to one single site in
501 Costa Rica, this is a first step on the development of more comprehensive approaches, which
502 take advantage of advanced technology to understand the effects of liana abundance on
503 tropical dry forest structure. The approach presented in this paper, presents important
504 contributions to efforts directed to estimate the potential effects of lianas on forest carbon in
505 secondary forests (*Durán and Sanchez-Azofeifa, 2015*), elements that seems not fully
506 considered yet in the tropical literature.
507

508 **Acknowledgements**
509 This work was carried out with the aid of a grant from the Inter-American Institute for
510 Global Change Research [IAI] CRN3 025 which is supported by the US National Science
511 Foundation [Grant GEO-1128040]. Logistical support by the University of Alberta is
512 acknowledged. We thank Ericka James her help during the process of data analysis. We
513 thank also Dr. Stefan Schnitzer for comments on earlier versions of the manuscript.
514

515 **References**

516 Arroyo-Mora, J.P., Sánchez□Azofeifa, G.A, Kalacska, M., Rivard, B., Calvo□Alvarado, J.,
517 and Janzen, D.: Secondary forest detection in a Neotropical dry forest landscape
518 using Landsat 7 ETM+ and IKONOS Imagery. Biotropica, 37 (4), 497-507, 2005
519 Arroyo-Mora, J. P., Sanchez-Asofeifa, G.A, Rivard, B., Calvo-Alvarado, J. C. and Janzen,
520 D. H.: Dynamics in landscape structure and composition for the Chorotega region,

Costa Rica from 1960 to 2000, Agriculture, Ecosystems & Environment , 106(1), 27–39, 2005.

Beland, M., Baldocchi, D. D., Widlowski, J.-L., Fournier, R. A. and Verstraete, M. M.: On seeing the wood from the leaves and the role of voxel size in determining leaf area distribution of forests with terrestrial LiDAR, Agriculture and Forest Meteorology 184, 82–97, 2014.

Calvo-Alvarado, J., B McLennan, GA Sánchez-Azofeifa, and T Garvin. Deforestation and forest restoration in Guanacaste, Costa Rica: Putting conservation policies in context. Forest Ecology and Management. 258(6), 931-940, 2009.

Canty, A. and Ripley B.: boot: bootstrap functions, available at: https://cran.r-project.org/web/packages/boot/ (last access: September 30, 2016), 2016.

Castillo, M., Rivard, B., Sánchez-Azofeifa, A., Calvo-Alvarado, J. and Dubayah, R.: LIDAR remote sensing for secondary Tropical Dry Forest identification, Remote Sens. Environ., 121, 132–143, 2012.

Castro-Esau, K., Sánchez-Azofeifa, G.A. and Caelli, T.: Discrimination of lianas and trees with leaf-level hyperspectral data, Remote Sens. Environ., 90 (3), 353–372, 2004.

Chen, Y.-J., Bongers, F., Cao, K.-F. and Cai, Z.-Q.: Above- and below-ground competition in high and low irradiance: tree seedling responses to a competing liana *Byttneria grandifolia*. J. Trop. Ecol., 24, 517–524, 2008.

Clawges, R., Vierling, L., Calhoon, M. and Toomey, M.: Use of a ground-based scanning lidar for estimation of biophysical properties of western larch (*Larix occidentalis*), Int. J. Remote Sens. 28 (19), 4331–4344, 2007.

Culvenor, D., Newnham, G., Mellor, A., Sims, N. and Haywood, A.: Automated In-Situ

Laser Scanner for Monitoring Forest Leaf Area Index, Sensors, 14(8), 14994–15008, 2014.

Dassot, M., Constant, T. and Fournier, M.: The use of terrestrial LiDAR technology in forest science.: Application fields, benefits and challenges, Ann. For. Sci., 68(5), 959–974, 2011.

Dewalt, S. J., Schnitzer, S. A. and Denslow, J. S.: Density and diversity of lianas along a chronosequence in a central Panamanian lowland forest, J. Trop. Ecol., 16(1), 1–19, 2000.

Durán, S.M. and Gianoli, E.: Carbon stocks in tropical forests decrease with liana density, Biol. Lett., 3–6, 2013.

Durán, S. M. and Sánchez-Azofeifa.: Liana effects on carbon storage and uptake in mature and secondary tropical forests, in: Biodiversity of lianas, edited by: Parthasarathy, N., pp. 43–55. Springer-Verlag, 2015.

Frazer, G.W., Canham, C.D., and Lertzman, K.P.: Gap light analyzer (GLA), Version 2.0: Imaging software to extract canopy structure and gap light transmission indices from true-colour fisheye photographs, users manual and program documentation. Simon Fraser University, BC and the Institute of Ecosystem Studies, NY, 1999.

Foster, J. R., Townsend, P. A. and Zganjar, C. E.: Spatial and temporal patterns of gap dominance by low-canopy lianas detected using EO-1 Hyperion and Landsat Thematic Mapper, Remote Sens. Environ., 112 (5), 2104–2117, 2008.

Freeman, E. A. and Ford, E.D.: Effects of data quality on analysis of ecological pattern using the *K (d)* statistical function. Ecology 83, 35–46.

González, I. and Déjean S.: CCA: canonical correlation analysis, available at: https://cran.r-project.org/web/packages/CCA/ (last access: September 30, 2016), 2015.Graham, E. A., Mulkey, S. S., Kitajima, K., Phillips, N. G. and Wright, S. J.: Cloud cover limits net CO2 uptake and growth of a rainforest tree during tropical rainy seasons., Proc. Natl. Acad. Sci. U. S. A., 100(2), 572–576, 2003.

van der Heijden, G.M.F, Schnitzer, S.A., Powers, J.S. and Phillips, O.L.: Liana Impacts on Carbon Cycling, Storage and Sequestration in Tropical Forests. Biotropica 45, 682–692, 2013.

van der Heijden, Powers, J.S., and Schnitzer, S.A.: Lianas reduce carbon accumulation and storage in tropical forests. PNAS 112, 13267-13271, 2015.

Hilje, B., Calvo-alvarado, J., Jiménez-rodríguez, C., Sánchez-azofeifa, A., José, S., Rica, C., Forestal, E. D. I., Rica, T. D. C. and Rica, C.: Tree species composition, breeding systems, and pollination and dispersal syndromes in three forest successional stages in a tropical dry forest in Mesoamerica, Trop. Conserv. Sci., 8(1), 76–94, 2015.

Jupp, D. L. B., Culvenor, D. S., Lovell, J. L., Newnham, G. J., Strahler, A. H. and Woodcock, C. E.: Estimating forest LAI profiles and structural parameters using a ground-based laser called "Echidna"., Tree Physiol., 29(2), 171–81, 2009.

Kalacska, M.: Leaf area index measurements in a tropical moist forest: A case study from Costa Rica, Remote Sens. Environ., 91(2), 134–152, 2004.

Kalacska, M. E. R., Sánchez-Azofeifa, G. A., Calvo-Alvarado, J. C., Rivard, B. and Quesada, M.: Effects of season and successional stage on leaf area index and spectral vegetation indices in three mesoamerican tropical dry forests, Biotropica, 37(4), 486–496, 2005.

589 Kalacska, M., Arroyo-Mora, JP., Soffer, R., Leblanc, G.: Quality control assessment of the
590 Mission Airborne Carbon 13 (MAC-13) hyperspectral imagery from Costa Rica.
591 Canadian Journal of Remote Sensing, 42, 85-105. 2016
592 Lefsky M., and McHale M..: Volumes estimates of trees with complex architecture from
593 terrestrial laser scanning. J Appl Remote Sens., 2, 023521, 2008.
594 Letcher, S. G. and Chazdon, R. L.: Lianas and self-supporting plants during tropical forest
595 succession, For. Ecol. Manage., 257 (10), 2150–2156, 2009.
596 Lovell, J. L., Jupp, D. L. B., Culvenor, D. S. and Coops, N. C.: Using airborne and ground-
597 based ranging lidar to measure canopy structure in Australian forests, Can. J. Remote
598 Sens., 29 (5), 607–622, 2014.
599 McGarigal, K.: Landscape pattern metrics, in Encyclopedia of environmetrics, vol 2. pp.
600 1135–1142, Wiley, Chichester,
601 Menzel, U.: CCP: Significance tests for canonical correlation analysis (CCA), available at:
602 https://cran.r-project.org/web/packages/CCP/ (last access: September 30, 2016),
603 2012.
604 Muss, J. D., Aguilar-Amuchastegui, N., Mladenoff, D. J. and Henebry, G. M.: Analysis of
605 Waveform Lidar Data Using Shape-Based Metrics, IEEE Geosci. Remote Sens. Lett.,
606 10 (1), 106–110, 2013.
607 Paul, G. S. and Yavitt, J. B.: Tropical Vine Growth and the Effects on Forest Succession: A
608 Review of the Ecology and Management of Tropical Climbing Plants, Bot. Rev.,
609 77 (1), 11–30, 2010.
610 Phillips, O., Martínez, R., Arroyo, L. and Baker, T.: Increasing dominance of large lianas in
611 Amazonian forests, Nature, 418, 770–774, 2002.

612 Phillips, O. L. and Lewis, S. L.: Recent changes in tropical forest biomass and dynamics,
613 For. Glob. Chang., 4, 77–108,2014.
614 Portillo-Quintero, C., Sanchez-Azofeifa, A. and Culvenor, D.: Using VEGNET In-Situ
615 monitoring LiDAR (IML) to capture dynamics of plant area index, structure and
616 phenology in Aspen Parkland Forests in Alberta, Canada, Forests, 5 (5), 1053–1068,
617 2014.
618 Quesada, M., Sanchez-Azofeifa, G. A., Alvarez-Añorve, M., Stoner, K. E., Avila-Cabadilla,
619 L., Calvo-Alvarado, J., Castillo, A., Espírito-Santo, M. M., Fagundes, M., Fernandes,
620 G. W., Gamon, J., Lopezaraiza-Mikel, M., Lawrence, D., Morellato, L. P. C., Powers,
621 J. S., Neves, F. D. S., Rosas-Guerrero, V., Sayago, R. and Sanchez-Montoya, G.:
622 Succession and management of tropical dry forests in the Americas: Review and new
623 perspectives, For. Ecol. Manage., 258 (6), 2009.
624 Quinn, G. P. and Keough M. J.: Experimental design and data analysis for biologists.
625 Cambridge University Press, New York, 443-472, 2002.
626 R Development Core Team: R: a language and environment for statistical computing,
627 available at: http://www.r-project.org (last access: September 30, 2016), 2016.
628 Ramírez, F. A., Armitage, R. P. and Danson, F. M.: Testing the application of terrestrial
629 laser scanning to measure forest canopy gap fraction, Remote Sens., 5 (6), 3037–
630 3056, 2013.
631 Richardson, J., Moskal, L. and Bakker, J.: Terrestrial Laser Scanning for Vegetation
632 Sampling, Sensors, 14 (11), 20304–20319, 2014.

633 Sánchez-Azofeifa, RC Harris, and DL Skole. Deforestation in Costa Rica: A quantitative
634 analysis using remote sensing imagery. Biotropica. 33(3), 378-384, 2001.

635 Sánchez-Azofeifa, G. A. and Castro-Esau, K.: Canopy observations on the hyperspectral
636 properties of a community of tropical dry forest lianas and their host trees, Int. J.
637 Remote Sens., 27 (10), 2101–2109, 2006.
638
639 Sánchez-Azofeifa, G. A., Kalácska, M., Espírito-Santo, M. M. Do, Fernandes, G. W. and
640 Schnitzer, S.: Tropical dry forest succession and the contribution of lianas to wood
641 area index (WAI), For. Ecol. Manage., 258 (6), 941–948, 2009.
642 Schnitzer, S. A and Bongers, F.: Increasing liana abundance and biomass in tropical forests:
643 emerging patterns and putative mechanisms., Ecol. Lett., 14 (4), 2011.
644 Schnitzer, S. A and Carson, W. P.: Lianas suppress tree regeneration and diversity in treefall
645 gaps., Ecol. Lett., 13 (7), 849–57, 2010.
646 Schnitzer, S. A., Dalling, J. W. and Carson, W. P.: The impact of lianas on tree regeneration
647 in tropical forest canopy gaps: evidence for an alternative pathway of gap-phase
648 regeneration, J. Ecol., 88 (4), 655–666, 2000.
649 Strahler, A. H., Jupp, D. L. ., Woodcock, C. E., Schaaf, C. B., Yao, T., Zhao, F., Yang, X.,
650 Lovell, J., Culvenor, D., Newnham, G., Ni-Miester, W. and Boykin-Morris, W.:
651 Retrieval of forest structural parameters using a ground-based lidar instrument
652 (Echidna ®), Can. J. Remote Sens., 34 (sup2), S426–S440, 2014.
653 Tymen, B., Réjou-Méchain, M., Dalling, J. W., Fauset, S., Feldpausch, T. R., Norden, N.,
654 Phillips, O. L., Turner, B. L., Viers, J. and Chave, J. Evidence for arrested succession
655 in a liana-infested Amazonian forest. J. Ecol. 104 (1), 149-159. 2016
656 Wright, S. J.: Tropical forests in a changing environment, Trends Ecol. Evol., 20(10), 553–
657 560, 2005.

Table 1. Mean (± SD) of parameters of forest structure extracted from plots with different successional stages and different relative abundance of lianas in the dry forest at Santa Rosa National Park, Costa Rica. Significant differences (*F-values* and their *p-values*) according to the successional stages, relative abundance of lianas and their interaction are represented by a posteriori ANOVA text extracted from MANOVA. DBH_{mean}, mean stem diameter at breast height (cm); TBA, total basal area (m^2); L/TBA, ratio of liana basal area to TBA.

Parameters	Early		Intermediate		ANOVA		
	LL	HL	LL	HL	Stage	Condition	Interaction
Stem density	1054 ± 370.72	1218.33 ± 603.24	1027.14 ± 379.02	1021 ± 331.54	0.55	0.15	0.27
DBH_{mean}	10.91 ± 2.36	11.83 ± 1.57	14.17 ± 1.85	11.56 ± 1.89	2.72	2.73	5.65*
TBA	1.44 ± 0.90	2.08 ± 1.01	2.61 ± 0.80	1.84 ± 0.61	1.39	0.48	5.15*
L/TBA (10^{-2})	0.38 ± 0.35	1.48 ± 0.84	0.35 ± 0.32	2.93 ± 2.14	2.76	14.11***	1.86

*, $p < 0.05$; ***, $p < 0.01$

668

669 Table 2. Mean (± SD) of parameters calculated by VEGNET system and HPs in plots
670 with different successional stages and different relative abundance of lianas in the dry
671 forest at Santa Rosa National Park, Costa Rica. Significant differences (*F-values* and
672 their *p-values*) according to the successional stages, relative abundance of lianas and
673 their interaction are represented by a posteriori ANOVA text extracted from MANOVA.
674 RG, radius of gyration; PAI, plant area index; $PAVD_{mean}$, plant area volume density;
675 H_{max}, maximum tree height (m); LAI, leaf area index.

Parameters	Early		Intermediate		ANOVA		
	LL	HL	LL	HL	Stage	Condition	Interaction
RG	4.21 ± 1.42	4.85 ± 0.92	4.69 ± 1.11	4.34 ± 0.91	0.03	0.01	1.41
C_x	0.19 ± 0.06	0.13 ± 0.04	0.14 ± 0.03	0.16 ± 0.04	0.12	0.14	5.95*
C_y	7.56 ± 2.96	8.43 ± 1.63	8.22 ± 2.07	7.56 ± 1.59	0.07	0.01	0.96
PAI	2.45 ± 0.28	2.10 ± 0.28	2.13 ± 0.34	2.31 ± 0.33	0.06	0.05	4.75*
$PAVD_{mean}$	0.19 ± 0.05	0.13 ± 0.04	0.14 ± 0.03	0.16 ± 0.04	0.14	0.22	7.26*
H_{max}	17.42 ± 5.51	18.17 ± 3.90	23.26 ± 7.73	18.01 ± 6.00	0.99	1.53	1.61
LAI	2.30 ± 0.32	2.46 ± 0.64	2.34 ± 0.46	2.92 ± 0.39	2.97	6.91*	1.32
Canopy openness	13.90 ± 3.94	12.59 ± 5.89	12.74 ± 5.27	8.67 ± 1.47	5.77*	6.78*	0.79

676 *, $p < 0.05$

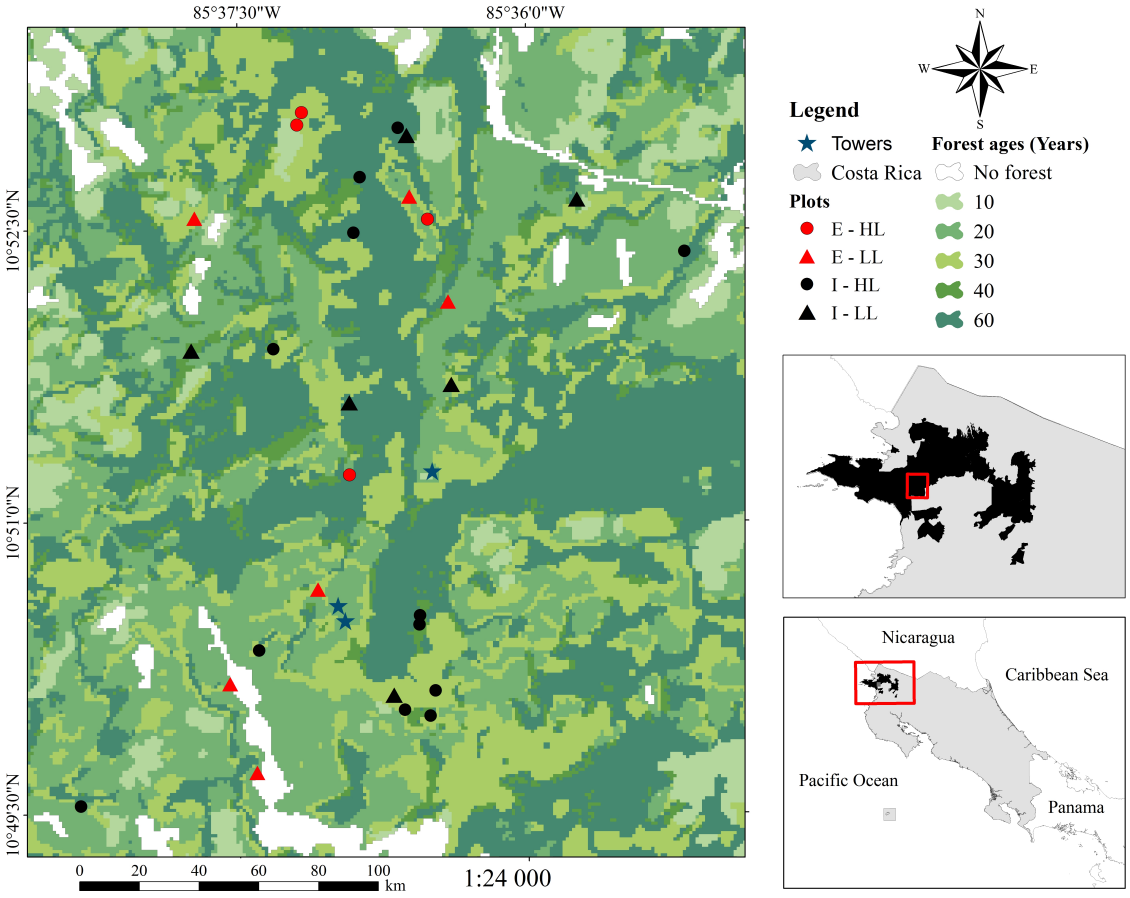

Figure 1. Localization of the sampled forest stands in Santa Rosa National Park Environmental Monitoring Super Site, Guanacaste, Costa Rica. Where E-HL indicate Early successional stage with a high relative abundance of lianas; E-LL Early successional stage with a low relative abundance of lianas; I-HL, Intermediate successional stage with a high relative abundance of lianas; I-LL, Intermediate successional stage with a low relative abundance of lianas. In addition, forests ages refer to: 60, forests detected since 1956; 40, forests detected since 1979; 30, forests detected since 1986; 20, forests detected since 1997; 10 forests detected since 2005, and no forest correspond to non-related to woodlands.

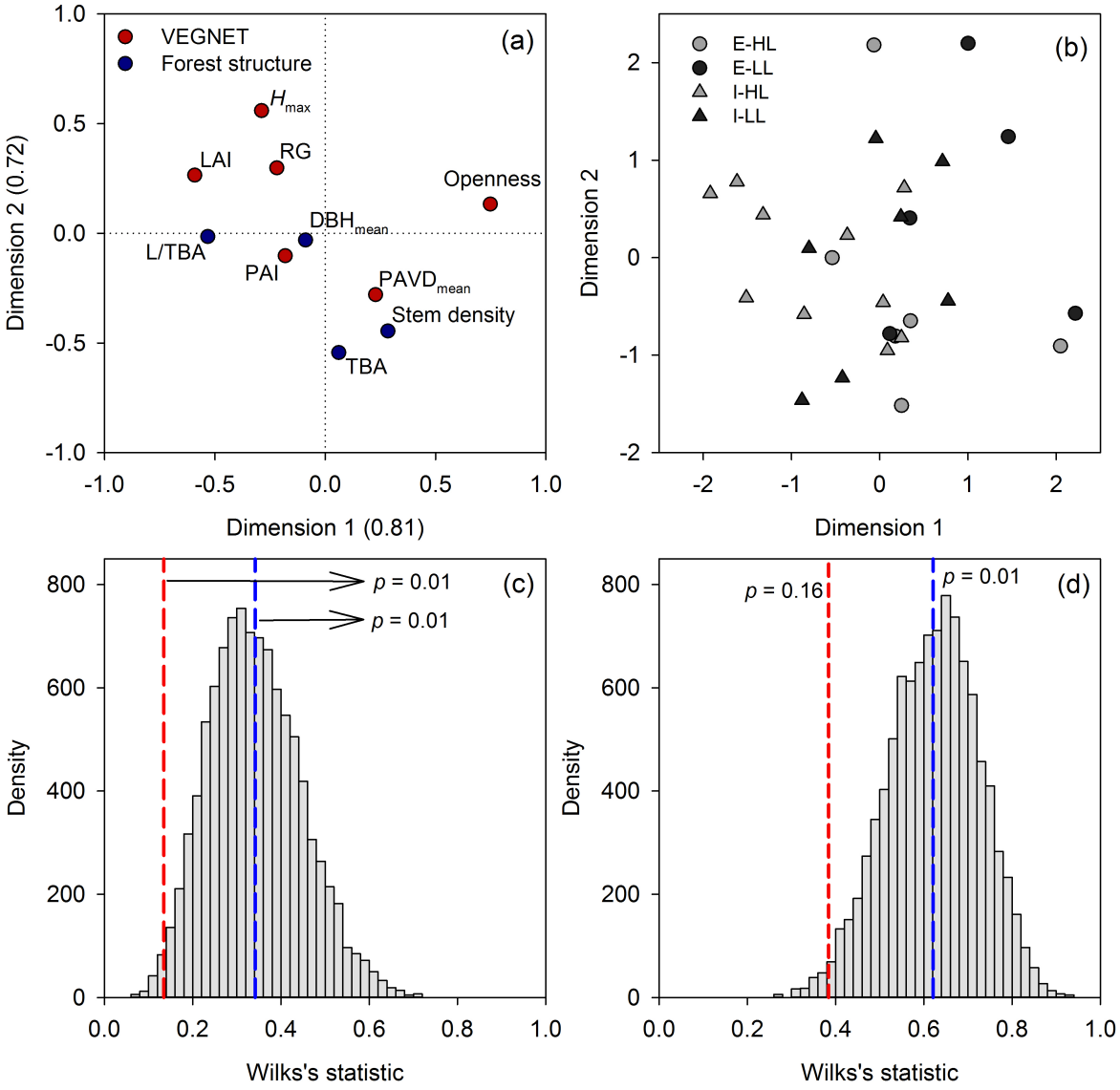

689

690 Figure 2. Canonical correspondence analysis to describe the association between the
691 parameters estimated by VEGNET system and the forest structure. a) VEGNET
692 coefficients are represented by red points, while forest structure coefficients are
693 represented by blue points. b) Individual scores of each plot of the canonical variates are
694 represented according to successional stages (E, early; I, intermediate) and relative liana
695 abundance (LL, low liana abundance; HL, high liana abundance). C and d represent the
696 permutation distribution of the Wilks' Lambda test to assign the statistical significance of

canonical correlation coefficients considering 4 and 3 canonical correlations, respectively; the red line represent the original value Wilks' Lambda, while the blue line represent the mean value permutated.

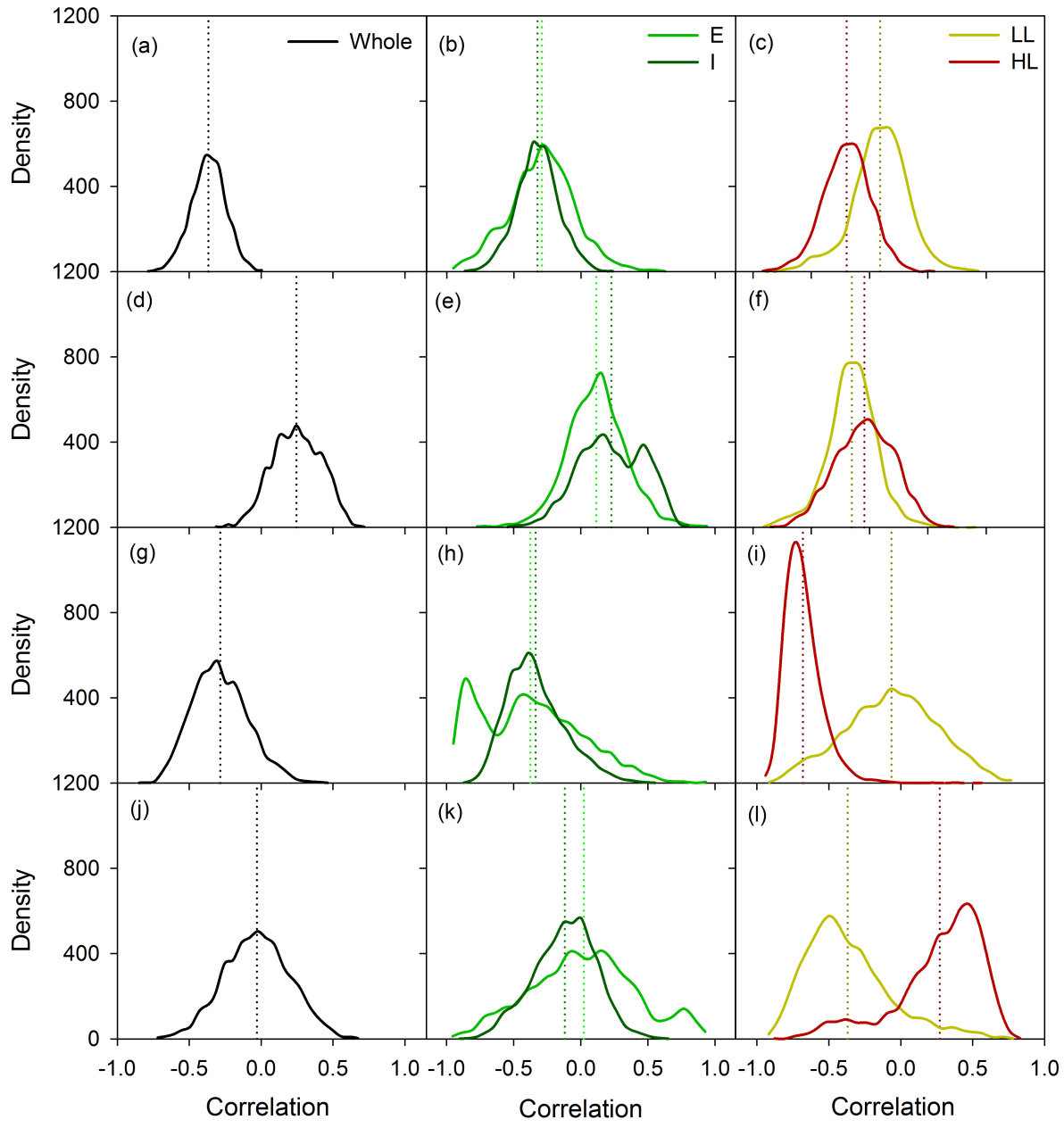

Figure 3. Density distribution of the bootstrapped correlation coefficients without and with distinction between successional stages (E, early; I, intermediate) and relative liana abundance (LL, low liana abundance; HL, high liana abundance). a, b, and c correspond to the correlation of canopy openness and the ratio of liana basal area (L) to total basal area (TBA); d, e, f correspond to leaf area index-L/TBA correlation; g, h, and i

707 correspond to the maximum tree height-TBA correlation; j, k, and l correspond to plant
708 area volume density-TBA correlation.
709
710
711
712
713
714